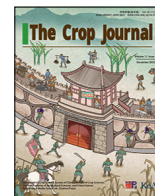




Contents lists available at ScienceDirect

The Crop Journal

journal homepage: www.keaipublishing.com/en/journals/the-crop-journal/

The MabHLH11 transcription factor interacting with MaMYB4 acts additively in increasing plant scopolin biosynthesis

Zhen Duan, Shengsheng Wang, Zhengshe Zhang, Qi Yan, Caibin Zhang, Pei Zhou, Fan Wu*, Jiyu Zhang*

State Key Laboratory of Herbage Improvement and Grassland Agro-ecosystems, Key Laboratory of Grassland Livestock Industry Innovation, Ministry of Agriculture and Rural Affairs, College of Pastoral Agriculture Science and Technology, Lanzhou University, Lanzhou 730020, Gansu, China

ARTICLE INFO

Article history:

Received 5 January 2023

Revised 16 June 2023

Accepted 27 June 2023

Available online 3 August 2023

Keywords:

Melilotus albus

Scopolin accumulation

Mabhlh11

Mamyb4

Maugt79

ABSTRACT

The plant natural product scopolin, a coumarin secondary metabolite, has been extensively exploited in flavor, cosmetic, medicine, and other industrial fields. *Melilotus albus*, a leguminous rotation crop, contains high concentrations of coumarin. The transcriptional regulatory network that controls the flow through the scopolin biosynthesis pipeline in *M. albus* remains poorly understood. MabHLH11 encodes a basic helix–loop–helix (bHLH) transcription factor whose transcription is positively associated with scopolin accumulation and with the expression of MaMYB4, the bHLH partner of the MYB–bHLH complex. Phylogenetic analysis grouped MabHLH11 in the TRANSPARENT TESTA 8 (TT8) clade of the bHLH IIIf subgroup. The MabHLH11 protein contained an MYB-interacting region and physically interacted with MaMYB4 in yeast and tobacco leaves. Co-overexpression of MabHLH11 with MaMYB4 in *M. albus* additively increased the expression of *UDP-glucosyltransferase* (*MaUGT79*) and induced more scopolin accumulation than occurred under the expression of MabHLH11 alone. MabHLH11 directly targeted the promoter of *MaUGT79* and the activation of MabHLH11 was strengthened by the presence of MaMYB4. Thus, MaMYB4 enhanced the function of MabHLH11 in upregulating scopolin biosynthesis in *M. albus*, providing a theoretical basis for scalable production of a high-value plant natural product.

© 2023 Crop Science Society of China and Institute of Crop Science, CAAS. Production and hosting by Elsevier B.V. on behalf of KeAi Communications Co., Ltd. This is an open access article under the CC BY-NC-ND license (<http://creativecommons.org/licenses/by-nc-nd/4.0/>).

1. Introduction

The coumarin glycoside scopolin is a secondary metabolite widely distributed among plant species and functions in plant development in scavenging reactive oxygen species (ROS) [1], shaping the composition of the root microbiome [2,3], resisting herbivorous insects [4], and facilitating nutrient uptake [5,6]. Scopolin is a potential bioactive compound for the treatment and prevention of obesity in humans [7] and is used in medical applications and the cosmetics industry [8]. Its pharmacological and synthetic biological prospects have aroused interest in pharmaceutical development and biosynthesis of plant secondary metabolites [9,10]. Scopolin is produced along with its related aglycone scopoletin and stored in vacuoles [11].

Scopolin is produced in the phenylpropanoid pathway. UDP-glucosyltransferase (UGT) is responsible for the final step in scopolin formation [12]. Scopolin biosynthesis branch of phenylpropanoid metabolism is tightly controlled and occurs essentially

at the transcriptional level [9,11,13]. Control of phenylpropanoid formation is exerted largely by the MYB–bHLH–WD40 transcription factor (TF) (MBW) complex to control the transcription of genes involved in synthesis by binding and activating their promoters, and can regulate pathway branches either positively or negatively [1,14,15].

A general MYB/bHLH model for regulation of scopolin pathway was found to operate in plants. The basic helix–loop–helix (bHLH), the second-largest TF family in plants, is divided into 12 subgroups [16]. bHLHs contain an MYB-interacting region (MIR) at the amino terminus, a WD40 repeat domain (WDR)-interacting region, and a conserved bHLH domain [17]. *Arabidopsis thaliana* MYB4 interacts with the bHLH TFs TT8, GL3, and EGL3 to interfere with the transcriptional activity of MBW complexes [18]. GmMYBA2 interacted with GmTT8a to directly activate anthocyanin biosynthetic genes via the MBW complex [19]. The role of the TF MYB4 in scopolin production has been documented [20]. The *Arabidopsis* bHLH TFs bHLH121 and bHLH29 regulate Fe-deficiency responses in a complex regulatory network indirectly modulating the expression of genes involved in Fe uptake, transport, and storage as well as in coumarin biosynthesis [21–24]. In one of the very few studies dealing with the regulation of scopolin production by bHLH [25], the

* Corresponding authors.

E-mail addresses: wufan@lzu.edu.cn (F. Wu), zhangjy@lzu.edu.cn (J. Zhang).

Arabidopsis TFs BRASSINOSTEROID ENHANCED EXPRESSION1 (BEE1)/G2-LIKE FLAVONOID REGULATOR (GFR) exerted control by interfering with the bHLH components TT8 and GL3 of the MBW complex to regulate scopolin biosynthesis under cold stress. However, little is known about the actual bHLH TFs that regulate flow through scopolin-biosynthesis pipelines in specialized plant metabolism, and the coordinated regulation partners have not been identified.

Melilotus albus is a rotation crop usually used for forage production and soil improvement [26], and is known for high tolerance of drought, cold and high-salinity environments [27]. It contains high concentrations of coumarin, ranging from 0.2% to 1.3% of dry matter [28]. The *M. albus* genome and transcriptomic data of near-isogenic lines (NILs) with various coumarin contents are available [29]. Differentially expressed unigenes and miRNAs involved in coumarin biosynthesis have been identified [30,31], and many transcription factors and gene family members have been found [29,32,33] to be implicated in the regulation of coumarin biosynthesis. There are still few studies on the transcriptional regulation of genes involved in the coumarin scopolin skeletons and there are still gaps in or knowledge of the function of bHLH in regulating scopolin biosynthesis. Clarifying the molecular function of bHLH may reveal the regulatory pathway of *M. albus* scopolin biosynthesis. Knowledge of the regulatory mechanisms of the scopolin pathway is likely to favor the development of new biotechnological tools for the generation of value-added plants with optimized scopolin content.

In this study, we attempt to better understand scopolin pathway regulation by bHLH/MYB transcriptional complex of *M. albus*. We report a bHLH TF MabHLH11, encoding a 659 amino acids protein localized in the nucleus, and the expression of which was correlated with scopolin biosynthesis. We confirmed the function of MabHLH11 by overexpression and RNAi knockdown assay. We investigated protein–protein interaction by yeast two-hybrid and bimolecular fluorescence complementation assays, the and special activations of proteins to target promoter to dissect the molecular mechanism underlying the MabHLH11-mediated regulation of scopolin biosynthesis.

2. Materials and methods

2.1. Plant materials and growth conditions

Melilotus albus NILs JiMa 46 and JiMa 49 [30] were grown in an incubator under controlled conditions (16 h/8 h day/night cycle at 25 °C, with relative humidity 40%). Roots, stems, leaves, and flowers at early flowering stage were collected, frozen in liquid nitrogen, and held at –80 °C until use. *Nicotiana benthamiana* plants used in this study were grown in pots in a growth chamber under a 16 h photoperiod with a 20 °C: 25 °C, night: day temperature.

2.2. Identification and classification of MabHLHs

The Hidden Markov Model (HMM) profile of the conserved structural domain of HLH (PF00010) retrieved from the Pfam database (<https://pfam.xfam.org/family/PF00010>) was used for identification of bHLH TF family genes in the *M. albus* genome by HMMER (v3.3.2) [34], with an E-value set to 10^{-2} . The genome sequences [29] of *M. albus* was obtained from College of Pastoral Agriculture Science and Technology, Lanzhou University. The putative MabHLH genes were submitted to CDD database (<https://www.ncbi.nlm.nih.gov/cdd/>) to retrieve the MabHLH gene family members eventually. The location information of all MabHLHs in the *M. albus* genome was extracted, and the MabHLHs on the corresponding chromosomal locations was displayed using TBtools [35]. The

MabHLHs were named based on their physical locations on chromosomes. The sequences of *A. thaliana* bHLH (AtbHLH) proteins, retrieved from the TAIR database (<https://www.arabidopsis.org/>), were included in multiple sequence alignments with MabHLH. An unrooted phylogenetic tree was constructed based on the alignments using MEGA 7.0 [36] with the neighbor-joining method, and bootstrap tests were performed using 1000 replicates to support statistical reliability. Subfamily grouping of MabHLH proteins was performed according to the classification of AtbHLH proteins [37].

2.3. Transcriptome analysis for tissue-specific expression

Transcript abundances of the 11 TT8 clade MabHLH genes in four tissues (roots, stems, leaves, and flowers) of *M. albus* were obtained from our previous study [33]. The *M. albus* gene expression levels were estimated based on fragments per kilobase of exon model per million mapped reads (FPKM) [38]. TBtools was used to construct a heat map of the MaTT8 gene expression profile.

2.4. MabHLH11 cloning and sequence analysis

A 1977-bp coding sequence (CDS) of MabHLH11 was PCR-amplified from cDNA of JiMa 46 and JiMa 49 using a Phanta Max Super-Fidelity DNA Polymerase (Vazyme, Nanjing, Jiangsu, China). For phylogenetic analysis, amino acid sequences of MabHLH11 were aligned with previously characterized bHLHs using ClustalX [39]. A phylogenetic tree was constructed from the alignments using MEGA 7.0 with the neighbor-joining method, and bootstrap tests were performed using 1000 replicates.

2.5. RNA extraction and gene expression analysis

Total RNA was extracted from leaves, stems, flowers, and roots at flowering stage and hairy roots of *M. albus* using the TransZol reagent (TransGen Biotech, Beijing, China). First-strand cDNA was obtained using the Hifair III 1st Strand cDNA Synthesis SuperMix for qPCR (gDNA digester plus) (Yeasen, Shanghai, China). Quantitative RT-PCR was performed using Hieff qPCR SYBR Green Master Mix (No Rox) (Yeasen) on a CFX96 Real-Time PCR Detection System (Bio-Rad, Los Angeles, CA, USA). β -tubulin was used as a reference gene. Relative expression levels were calculated relative to controls using the $2^{-\Delta\Delta CT}$ method [40]. There were three biological replicates for all analyses. Primers used for qRT-PCR are listed in Table S1.

2.6. Subcellular localization

To investigate the subcellular localizations of the MabHLH11, we constructed recombinant MabHLH11 tagged at the N-terminus with red fluorescent protein (RFP), and the CDS of MabHLH11 was cloned into the binary vector pBI121 DsRed2 driven by the 35S promoter. The specific primers are listed in Table S1. *Agrobacterium tumefaciens* GV3101 carrying 35S:-MabHLH11-RFP and the control vector with RFP alone were transformed into the healthy leaves of 6-week-old *N. benthamiana* seedlings. The nuclear marker pBI121-NLS-CFP was co-transformed into the *N. benthamiana* leaves to identify the location of the nucleus. The system was subsequently cultured in the dark for one day and then placed into a growth chamber for another two days [41]. A laser scanning confocal microscope (Olympus FV3000, Japan) was used to acquire images of transformed leaves.

2.7. Prediction of protein–protein interactions of MabHLH11 protein

Protein–protein interactions of MabHLH11 protein were predicted with STRING 11.5 (<https://cn.string-db.org/>) [38].

2.8. Yeast two-hybrid assay

The full-length cDNA of MaMYB4 was introduced into pGADT7 and that of MabHLH11 was introduced into pGBKT7 using the ClonExpress MultiS One Step Cloning Kit (Vazyme). The primers used for plasmid construction are listed in Table S1. Pairs of constructs with bait and prey plasmids were cotransformed into the AH109 yeast strain. SD-medium lacking Trp/Leu was used to identify positive strains carrying both pGADT7 and pGBKT7. Positive transformants were spotted on SD-medium lacking Trp/Leu/His/Ade at several dilutions and cultured for three days at 30 °C for interaction detection [41].

2.9. Bimolecular fluorescence complementation assay

The coding regions of MabHLH11 and of the MaMYB4 C-terminus were cloned into the pSAT1-nVenus-C(pE3242) and pSAT1-cCFP-C(pE3242) vectors, respectively. The recombinant vectors or control (empty vectors) were transformed into *A. tumefaciens* GV3101 and then co-transformed into *N. benthamiana* leaves with infiltration buffer [42]. GFP signal was detected by laser scanning confocal microscopy 48 h after infiltration.

2.10. Hairy root initiation

To produce the MabHLH11, MaMYB4, and MabHLH11+MaMYB4 co-overexpression constructs, full-length cDNAs of MabHLH11 and MaMYB4 were cloned into pBI 121 binary vectors, using the ClonExpress Kit. The constructs were introduced into *Agrobacterium rhizogene* K599 strain by electroporation. Transgenic hairy roots were obtained following the protocol, described elsewhere [43]. Transgenic lines transfected with empty vector (EV) were used as control. Screening of transformed hairy roots was performed by observation of RFP signal, which was used as a transformation marker, by qRT-PCR to detect and quantify the MabHLH11 transcript level. Hairy roots were harvested for determination of scopolin content.

2.11. Scopolin extraction and quantification

Ambient temperature-dried leaves from fresh samples were ground and passed through a sieve with a mesh size of 0.45 mm and extracted with an ethanol/water mixture (80: 20, v/v). For leaf extraction, 50 mL of solvent g⁻¹ of dry weight was used. For hairy root extraction, 5 mL 80% ethanol per 100 mg was added to the frozen material [1]. After shaking for 10 min, ultrasonic extraction was performed at room temperature for 60 min. The ratio of the weight of the fresh samples to the volume of the extraction solution was the same for all the samples in a given experiment. The extracts were filtered through 0.45 µm filters for high-performance liquid chromatography (HPLC) separation.

HPLC was performed with an Agilent 1100 HPLC system using a 5 µm C18 column (4.6 mm × 150 mm, Agilent-XDB), maintained at 30 °C, with water (containing 0.1% phosphorous acid) and acetonitrile as mobile phase. The flow rate of the mobile phase was set to 1 mL min⁻¹ for 20 min. The chromatogram based on detection at a wavelength of 346 nm was used for scopolin identification and quantification.

2.12. Yeast one-hybrid assay

For the Matchmaker Gold yeast one-hybrid system (Clontech, Mountain View, CA, USA), the MabHLH11 CDS was fused to the GAL4 transcription factor activation domain (GAL4AD) in the pGADT7 vector to generate the prey vector (pGADT7-MabHLH11). The various promoter fragments of *MaUGT79* (2.0-kb) were inserted into the pAbAi vector to construct the baits (*pro1/2/3/4/5MaUGT79-AbAi*). These *Bst*I I-cut bait constructs were integrated separately into the genome of Y1HGOLD to generate five bait reporter strains. The minimal inhibitory concentrations of Aureobasidin A (AbA) were determined for the baits using SD/-Ura agar plates containing 0–1000 ng mL⁻¹ AbA. After selection of the transformants on SD/-Ura plates, the pGADT7-MabHLH11 construct was introduced into the bait reporter strains, with a blank pGADT7 plasmid serving as a negative control. Positive transformants were selected on SD/-Leu medium supplemented with an appropriate concentration of AbA and cultured at 30 °C for 3 d [44].

2.13. Dual-luciferase assay

For the dual-luciferase (Dual-LUC) assay, the *MaUGT79* promoter was ligated into pGreenII-0080-LUC to generate the reporter construct *proMaUGT79:LUC*. The MabHLH11 and MaMYB4 were ligated into the binary vector pBI121 to generate the effector construct 35S:MabHLH11 and 35S:MaMYB4. The effector and reporter constructs were transformed separately into *A. tumefaciens* strain GV3101 harboring pSoup helper vector, which was used to co-infect 6-week-old *N. benthamiana* leaves. Leaves infiltrated with the pBI121 and *proMaUGT79:LUC* were used as control [44]. The system was subsequently cultured in the dark for 12 h and then placed into a growth chamber for another two days. A Fluorescence Chemiluminescence Imaging System (FX6.EDGE Spectra; VILBER, France) was used to capture the LUC image. The promoter activities were determined by measuring firefly luciferase to renilla luciferase (LUC/REN) ratios using the Dual Luciferase Reporter Gene Assay Kit (Beyotime, Shanghai, China) with a Multimode Reader (Varioskan LUX, Thermo Fisher Scientific, Finland). Five biological replications were measured for each sample.

3. Results

3.1. Expression of MabHLH11 was correlated with scopolin biosynthesis

A total of 148 bHLH TF family genes were identified in the *M. albus* genome. The MabHLHs were renamed from MabHLH1 to MabHLH148 based on the gene distribution information on the chromosomes (Fig. S1). A phylogenetic tree was constructed using 173 AtbHLHs from *Arabidopsis* and 148 MabHLHs from *M. albus* to investigate the potential evolutionary relationships of MabHLH members. These bHLHs were classified into 12 major groups (subfamilies I to XII) (Fig. S2). Eleven TT8 members harboring a highly conserved bHLH-MYC_N protein domain (PF14215.7) were identified among the 148 bHLH genes. The transcript abundance of the 11 TT8 members was evaluated in the four tissues to determine whether their expression patterns coincided spatially with scopolin accumulation. As shown in Fig. 1A, the highest content of scopolin was found in flowers in both JiMa 46 and JiMa 49 and the content of JiMa 49 was significantly higher than that of JiMa 46. RNA-seq data showed that the transcript abundance of MabHLH11 was highest in flowers, as was scopolin content (Fig. 1B). The qRT-PCR assay showed that the expression pattern of MabHLH11 in JiMa 46 showed expression trends similar to those shown in the

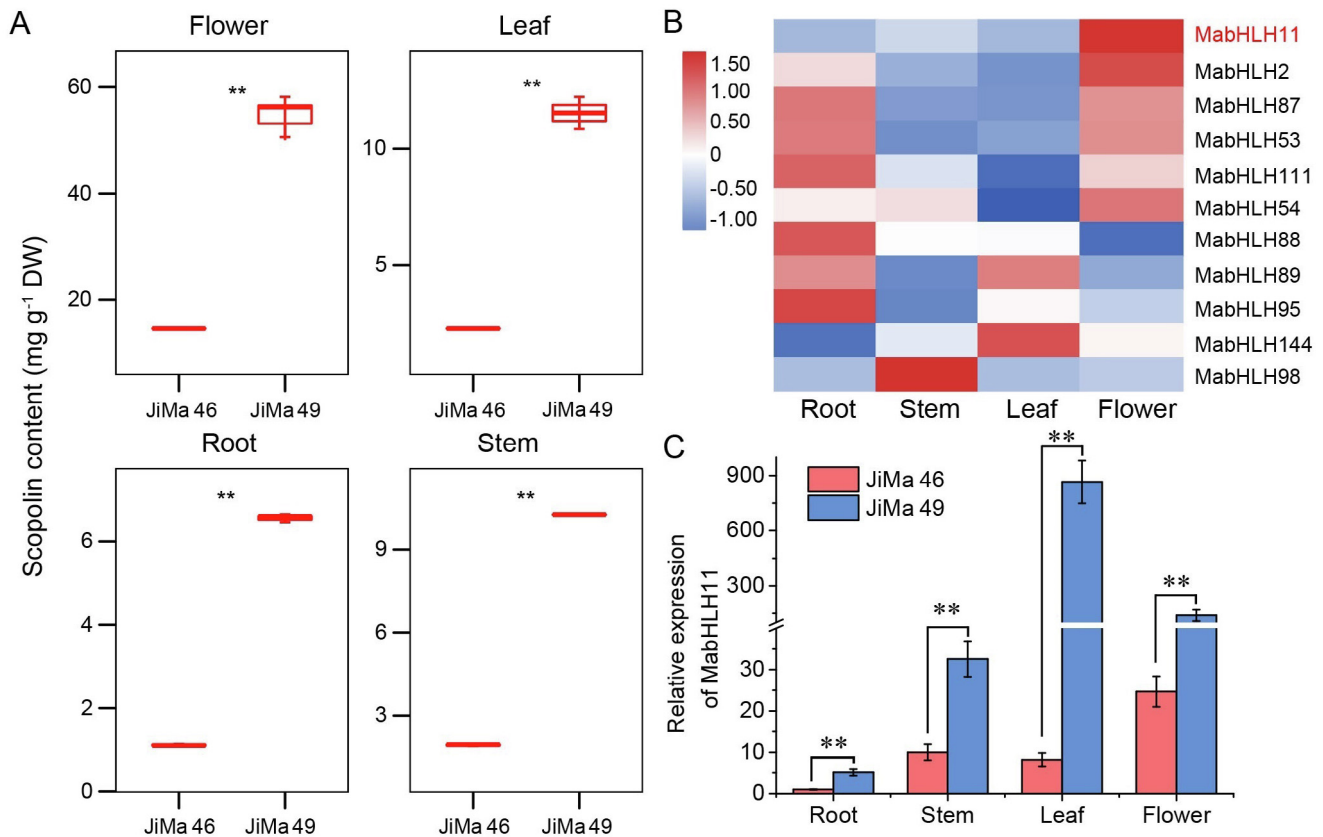


Fig. 1. Scopolin contents and expression pattern of MabHLH11. (A) Scopolin contents in four tissues of JiMa 46 and JiMa 49. (B) Expression values (FPKM) of 11 TT8 transcription factors in tissues of JiMa 46 from RNA-seq data. (C) qRT-PCR analysis of MabHLH11 in tissues of JiMa 46 and JiMa 49. Error bars represent SD ($n = 3$). Significant differences were detected by Student's t -test, **, $P < 0.01$.

RNA-seq data, and the expression of the MabHLH11 gene in tissues of JiMa 49 showed significantly higher expression level than that in JiMa 46 (Fig. 1C), indicating that the expression patterns of MabHLH11 were correlated with scopolin biosynthesis.

3.2. MabHLH11 containing an MYB-interacting region

The 1977-bp full-length cDNA of MabHLH11 was isolated and sequenced to verify the open reading frame (ORF) and no polymorphisms were detected in the MabHLH11 gene between the NILs JiMa 46 and JiMa 49. It encoded a peptide of 659 amino acids with a molecular mass of 73.86 kDa and a pI of 5.25 and harbored a conserved bHLH domain and an MYB-interacting region (MIR) domain. Alignment of the deduced amino acid sequence of MabHLH11 with bHLH proteins in other plant species (MtTT8 in *Medicago truncatula*, MdbHLH3 in *Malus domestica*, VvMYC1 in *Vitis vinifera*, PhAN1 in *Petunia hybrida*, and AtTT8 in *Arabidopsis thaliana*) revealed an N-terminal MIR at 11–187 aa and a conserved bHLH domain at 460–509 aa (Fig. S3). The conserved MIR domain is a prerequisite for the formation of MBW activation complexes. A phylogenetic tree was constructed using full-length amino acid sequences of MabHLH11 and 22 other bHLH proteins (Fig. 2). MabHLH11 was placed in subgroup IIIc clade B (Figs. S2), close to the branches of AtTT8 and AtGL3, which could be the candidate ortholog (Fig. 2). Phylogenetic analyses further indicated that MabHLH11 was a candidate regulatory gene with a function similar to that of AtTT8 and AtGL3 in the scopolin biosynthetic pathway.

3.3. MabHLH11 is located in the nucleus

MabHLH11 must enter the nucleus of plant cells to function as a TF. A nuclear localization signal peptide (NLS, 469–497 aa) was identified in the predicted MabHLH11 protein (Fig. S3). To determine the subcellular localization of MabHLH11, we expressed the MabHLH11-RFP fusion protein under the control of the 35S promoter in the leaves of *N. benthamiana*. It appeared that the MabHLH11-RFP fusion protein was localized in the nucleus in perfect coincidence with nuclear markers, whereas GFP could be found throughout the cells of tobacco leaves (Fig. 3), a finding consistent with its putative role as a transcription factor in the nucleus.

3.4. MabHLH11 physically interacted with MaMYB4

As putative transcriptional regulators, bHLH proteins interact with MYB TFs to compose the MBW complex. Previous experiments [18] showed that *A. thaliana* bHLH transcription factors AtTT8 interact with MYB4 and thereby interfere with the transcriptional activity of the MBW complexes. Prediction of protein–protein interactions of MabHLH11 protein with reference to the protein–protein interactions of the TT8 protein of *A. thaliana* showed the same result (Fig. S4), leading us to hypothesize that MabHLH11 interacts with MaMYB4. To investigate this hypothesis, two different methods were employed. First, yeast two-hybrid assays were performed to investigate whether MabHLH11 interacted with MaMYB4. A full-length MabHLH11 protein was found to interact with MaMYB4 directly in yeast (Fig. 4B). To confirm this

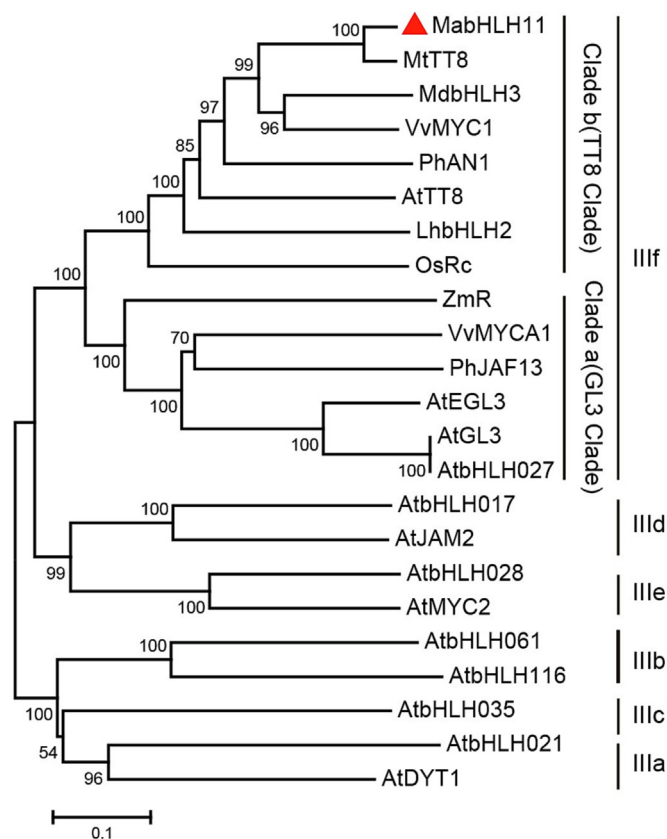


Fig. 2. A neighbor-joining phylogenetic tree of bHLH subfamilies III TFs. Amino acid sequences were retrieved from GenBank with the following accession numbers: AtTT8 (Q9FT81), AtGL3 (NP_680372), AtEGL3 (Q9CAD0), AtbHLH061 (AAM10950), AtbHLH116 (AAL84972), AtDYT1 (O81900), AtbHLH021 (NP_179283), AtbHLH027 (AAS79544), AtbHLH035 (NP_974948), AtJAM2 (Q9LNJ5), AtbHLH017 (AAM19778), AtMYC2 (Q39204), and AtbHLH028 (AAL55721) in *Arabidopsis thaliana*; and MdbHLH3 (ADL36597) in *Malus domestica*; VvMYCA1 (ABM92332) and VvMYC1 (ACC68685) in *Vitis vinifera*; MtTT8 (KM892777) in *Medicago truncatula*; OsRc (ABB17166) in *Oryza rufipogon*; PhAN1 (AAG25928) and PhJAF13 (AAC39455) in *Petunia hybrida*; LhbHLH2 (BAE20058) in *Lilium hybrid*; and ZmR (P13027) in *Zea mays*. The numbers next to the nodes are bootstrap values from 1000 replications.

interaction, a BiFC experiment was selected as a method for an *in vivo* assay using a cell biology approach. MabHLH11 and MaMYB4 proteins were fused to the C-terminus of cCFP (cCFP-MaMYB4) and nVenus (nVenus-MabHLH11), respectively, and then transiently transformed into *N. benthamiana* leaves. The YFP signal localized to the nucleus, showing close interaction between MabHLH11 and MaMYB4 as well as nuclear localization (Fig. 4C).

3.5. Overexpression of MabHLH11 and MaMYB4 results in scopolin biosynthesis in *m. Albus*

The expression levels of MabHLH11 and MaMYB4 were measured in four tissues of JiMa 49. qRT-PCR analysis showed that MabHLH11 expression was highly correlated with MaMYB4 expression (Fig. 5A). To further characterize the regulation role of MabHLH11 and MaMYB4 in scopolin biosynthesis, we performed overexpression experiments using *A. rhizogenes*-mediated transformation of hairy roots. The transgenic hairy roots were identified by RFP signal detection and qRT-PCR. Strong RFP signal was observed in positive OE-MabHLH11 and OE-MabHLH11+OE-MaMYB4 transgenic hairy roots (Fig. 5B), and the relative expression of MaMYB4 showed a marked increase in positive OE-MaMYB4 and OE-MabHLH11+OE-MaMYB4 transgenic hairy roots, and did not increase in OE-MabHLH11 transgenic hairy roots (Fig. 5C). The relative expression of MabHLH11 showed a marked increase in posi-

tive OE-MabHLH11 and OE-MaMYB4 transgenic hairy roots and greater increase in OE-MabHLH11+OE-MaMYB4 positive hairy roots (Fig. 5D), suggesting that MaMYB4 is an upstream regulator. The positive transgenic hairy roots of overexpressing MaMYB4 (OE-MaMYB4), overexpressing MabHLH11 (OE-MabHLH11) and co-overexpressing MabHLH11 and MaMYB4 (OE-MabHLH11+OE-MaMYB4) were selected for functional characterization, with hairy roots transfected with the empty vector used as control (EV). Endogenous total scopolin from OE-MaMYB4, OE-MabHLH11 and OE-MabHLH11+OE-MaMYB4 lines was extracted and quantified by HPLC. Scopolin accumulation in OE-MabHLH11 lines was much higher than that of EV (Fig. 5F), indicating that upregulated expression of MabHLH11 increased scopolin accumulation in *M. albus*. Scopolin levels were sharply increased by MabHLH11 and MaMYB4 co-expression (Fig. 5D), suggesting an additive effect of MabHLH11 and MaMYB4. As shown in Fig. 5, the expressions of *MaUGT79* (F) and *MaCCoAOMT* (G) were markedly increased in MabHLH11-MaMYB4-co-expression lines relative to those in EV, suggesting an additive effect of MabHLH11 and MaMYB4 in up-regulation of scopolin biosynthesis genes. These findings suggested that MabHLH11 and MaMYB4 function in scopolin accumulation.

3.6. MabHLH11 bound to the promoter of *MaUGT79*

To investigate whether MabHLH11 was involved in the transcriptional regulation of *MaUGT79*, yeast one-hybrid assay was performed. The promoter of *MaUGT79* was isolated from JiMa 49 and the predicted MYB-recognizing element (MRE) and the bHLH-recognizing element (BRE) were identified. We found 3 MYC *cis*-acting elements in the promoter of *MaUGT79*: CATGTG at -1234 bp, CATGTG at -1343 bp, and CATTGG at -1828 bp in the *MaUGT79* promoter right on P1 and P2 (Fig. S5). A 2000-bp DNA sequence upstream of the *MaUGT79* start codon was separated into five parts: P1 (-2000 to -1589), P2 (-1609 to -1201), P3 (-1229 to -900), P4 (-926 to -203), and P5 (-225 to -1, Fig. S5A). The P1, P2, P3, P4 and P5 sequences were integrated individually into the genomes of yeast cells. Introducing pGADT7-MabHLH11 into each of the yeast strains revealed that the P4 and P5 sequences of the *MaUGT79* promoter were not suitable for the Y1H system because 1000 ng mL⁻¹ AbA was still unable to suppress the basal expression in the Y1H Gold harbouring *P4MaUGT79*-AbAi and *P5MaUGT79*-AbAi (Fig. S5B), and then only two strains, carrying the P1 and P2 promoter, grew on selective media (Fig. 6B). This finding indicated that MabHLH11 binds to the P1 and P2 fragments of the *MaUGT79* promoter.

3.7. MabHLH11 interacted with MaMYB4 to activate *MaUGT79*

The regulatory roles of MabHLH11 and MaMYB4 in scopolin accumulation were further examined by determining promoter activation using a dual-luciferase system in tobacco leaves. We first investigated whether the promoter of *MaUGT79* contained *cis*-elements bound by MBW complexes. As shown in Fig. 7A, the promoter region of *MaUGT79* contains binding elements of bHLH and MYB. Then the *MaUGT79* promoter was tested, being activated and binding directly to MabHLH11 and MaMYB4. MabHLH11 increased luciferase activity 1.60-fold and MaMYB4 increased luciferase activity 2.39-fold (Fig. 7C). The activation effects of *MaUGT79* promoter were strengthened by co-expression of MabHLH11 and MaMYB4 in comparison with that of MabHLH11 or MaMYB4 alone and luciferase activity was strongly (3.78-fold) increased. Co-expression with the MabHLH11 plus MaMYB4 transcription factor produced a strong LUC signal (Fig. 7C). These findings demonstrated that MabHLH11 interacting with MaMYB4 directly activated the promoter of scopolin structural gene *MaUGT79* to upregulate scopolin accumulation.

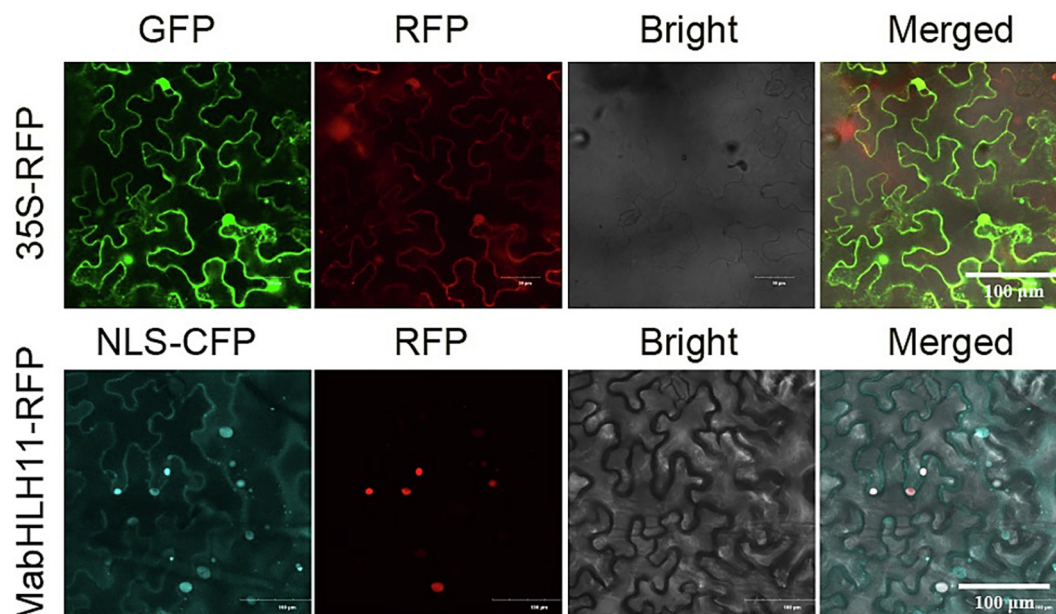


Fig. 3. Subcellular localization of MabHLH11 in *Nicotiana benthamiana* leaves. MabHLH11 was fused to RFP. NIS-CFP served as a marker for the nucleus. The fluorescence was observed under a confocal laser scanning microscope. Scale bars, 100 μm.

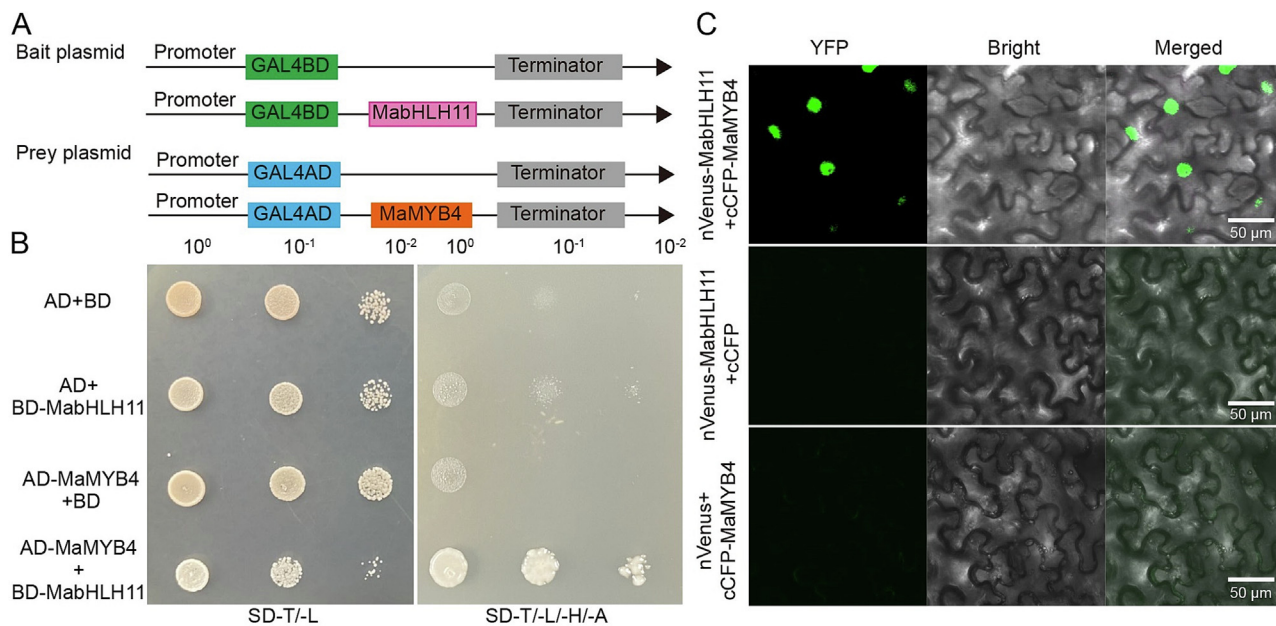


Fig. 4. MabHLH11 interacted with MaMYB4. (A) Schematic diagram of yeast two-hybrid assay. (B) The coding region of MabHLH11 was cloned into a BD plasmid (pGBKT7), the MaMYB4 was inserted to an AD plasmid (pGADT7), and plasmids were co-transformed into yeast strain AH109. MabHLH11 and MaMYB4 were used as negative controls. The cotransformed yeast cells were grown and monitored on SD/-Trp/-Leu (-T/-L) medium, and SD/-Trp/-Leu/-His/-Ade (-T/-L/-H/-A) media. (C) Bimolecular fluorescence complementation (BiFC) confirmed the specificity of interaction between MabHLH11 and MaMYB4 in *N. benthamiana* leaves. Full-length MaMYB4 was transformed into pSAT1-cCFP-C(pE3228) and full-length MabHLH11 was inserted into pSAT1-nVenus-C(pE3242). The two vectors were coexpressed in *N. benthamiana* leaves. Scale bars, 50 μm.

4. Discussion

4.1. Conserved clade IIIf MabHLH11 plays an important role in regulating scopolin accumulation in *m. Albus*

Limited information is available about TFs implicated in the activation of specialized scopolin metabolite production. In our study, we identified a MabHLH11 TF, the transcription pattern of MabHLH11 was correlated with the accumulation of scopolin (Fig. 1). MabHLH11 belonged to subfamily IIIf clade b (Fig. S2)

and was most similar to AtTT8 and AtGL3 (Fig. 2). Most subfamily III members are involved in the regulation of flavonoid biosynthesis, and contain an MIR at the amino terminus, a WDR, and a conserved bHLH domain [45]. Our findings that MabHLH11 contained an N-terminal MIR at the first 11–187 amino acids and a conserved bHLH domain at 460–509 amino acids (Fig. S3) are consistent with this structure. A previous study [37] showed that members of bHLH subfamily III associate with R2R3-MYB proteins, in a similar way to our study, the MabHLH protein MabHLH11, which interacts with the R2R3-type MYB protein MaMYB4.

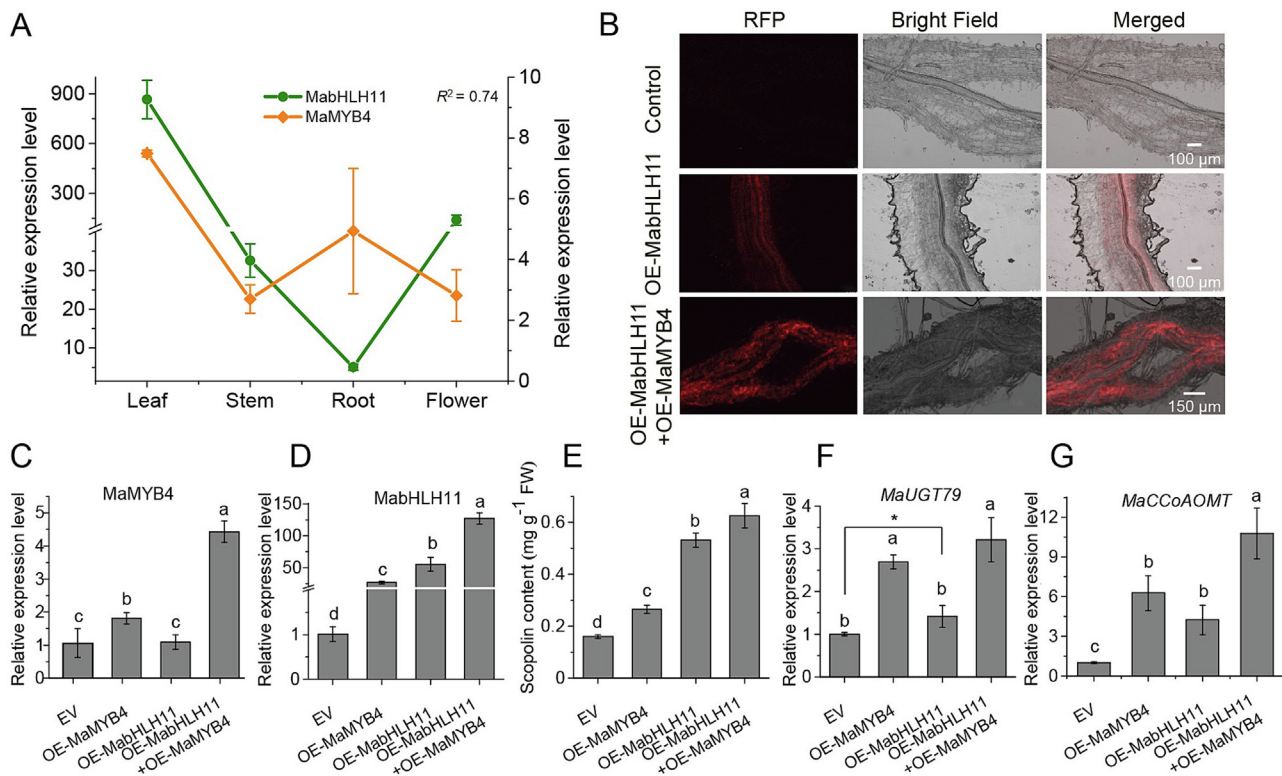


Fig. 5. MabHLH11 coupled with MaMYB4 to activate scopolin accumulation in *M. albus*. (A) The correlation between the expression of MabHLH11 and MaMYB4 in four tissues at the same developmental stage of JiMa 49. (B) RFP signals in OE-MabHLH11 and OE-MabHLH11+OE-MaMYB4 in transgenic *M. albus* hairy roots. Scale bars, 100 μ m (upper panels) and 150 μ m (bottom panel). (C) Co-overexpression of MabHLH11 and MaMYB4 to modulate scopolin synthesis in an additive manner in *M. albus* hairy roots. (C–G) qRT-PCR analysis of MabHLH11 (C), MabHLH11 (D), *MaUGT79* (F) and *MaCCoAOMT* (G) and scopolin content (E) in hairy roots of EV (transfected with empty vector), OE-MaMYB4, OE-MabHLH11 and co-overexpression MabHLH11 and MaMYB4 (OE-MabHLH11+OE-MaMYB4) lines. qRT-PCR was performed to detect gene expression levels. Values are normalized to β -*tubulin*. Error bars represent \pm SD with three technical repeats for each experimental group. Differing letters above bars indicate differences ($P < 0.05$) by one-way ANOVA. Significant differences were detected by Student's *t*-test (*, $P < 0.05$).

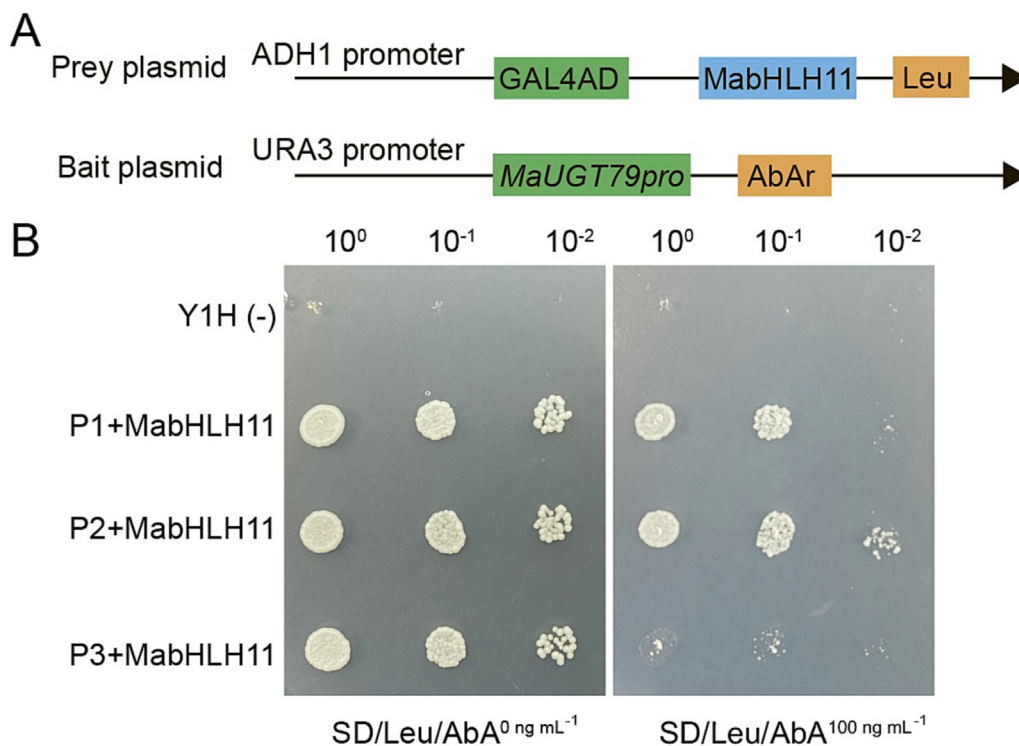


Fig. 6. The promoter of *MaUGT79* is the direct target by MabHLH11. (A) Schematic diagram of the prey plasmid and bait plasmid in yeast one-hybrid (Y1H) assay. The promoter fragment of *MaUGT79* was cloned into the pAbAi vector to generate the bait plasmid and the prey plasmid was generated by recombining the MabHLH11 into the pGADT7 vector. (B) Yeast one-hybrid assay. A pair of plasmids, pAbAi containing different fragments of the *MaUGT79* promoter and pGADT7 containing MabHLH11 were introduced into yeast strain Y1H gold and cultured on SD medium without Leu containing several concentrations of AbA at 30 °C for 3 days.

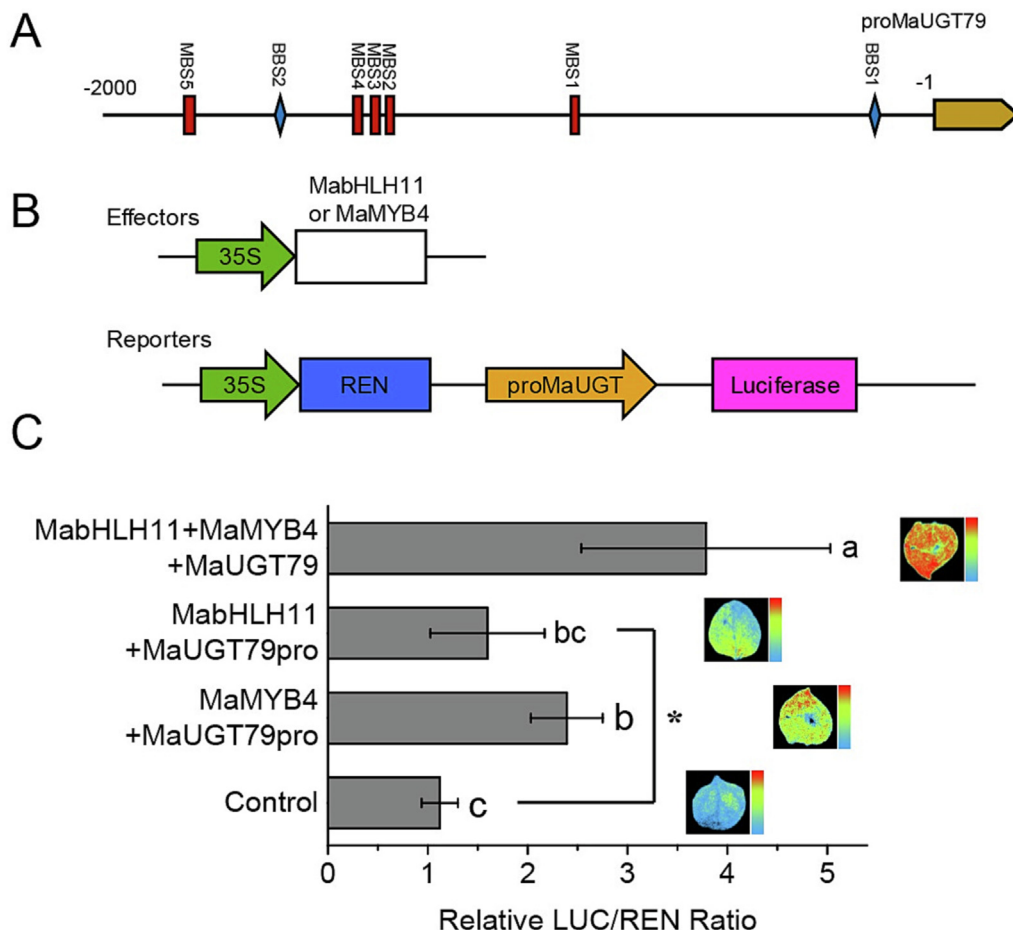


Fig. 7. MabHLH11 interacted with MaMYB4 to activate the *MaUGT79* promoter. (A) Schematic diagram of the *MaUGT79* promoter. Putative *cis-acting* elements are indicated: MBS (red), MYB binding sites; G-box elements (yellow), bHLH binding sites (BBS). (B) Schematic of effector and reporter construct containing the luciferase (*LUC*) reporter gene driven by the *MaUGT79* promoter and the renilla luciferase (*REN*) gene driven by the CaMV 35S promoter as a control for normalization. (C) Dual-luciferase (*LUC*) assay in *Nicotiana benthamiana* leaves showing the effects on transcription of *MaUGT79* by MabHLH11 and MaMYB4 individually or collectively (representative photographs are on the right and detected *LUC*/renilla luciferase (*REN*) activity is on the left). Error bars represent \pm SD with five technical repeats for each experimental group. Different letters beside bars indicate differences ($P < 0.05$) by one-way ANOVA. Significant differences were detected by Student's *t*-test (*, $P < 0.05$).

We found the MabHLH11 promoter does not harbor a DNA transposon or single nucleotide polymorphism (SNP), and no other polymorphisms were detected in the MabHLH11 gene between the JiMa 46 and JiMa 49. In addition, the reduced expression of MabHLH11 in JiMa 46 relative to that in JiMa 49 (Fig. 1C), suggested that the transcription pattern of MabHLH11 was independent of the genotype but correlated with the accumulation of scopolin, and that other genes might regulate the expression of MabHLH11. Therefore, we postulate that MabHLH11 may contribute to scopolin accumulation in *M. albus*. To further confirm its regulatory role, the overexpression and RNAi of MabHLH11 were performed in *M. albus* hairy root. As expected, overexpression MabHLH11 can induce significant scopolin accumulation by upregulating the transcription abundance of scopolin-related genes (Fig. 5E–G). The dual-luciferase assays suggest that the promoter of *MaUGT79* is activated by MabHLH11 (Fig. 7C). These findings suggest that MabHLH11 has strong activating ability for promoter of *MaUGT79*. This behavior is similar to triterpene saponin-related bHLH [46]. Taken together, these results indicate that MabHLH11 plays a critical role in regulating scopolin accumulation by increasing the promoter activity of *MaUGT79*.

4.2. MabHLH11 functioned in regulation of scopolin accumulation by interacting with MaMYB4

A previous study [25] showed that flavonoid synthesis is regulated predominantly by MYB and bHLH TFs. In our study, MabHLH11 harbored a MYB binding site in its amino acid sequence (Fig. S3). The bHLH proteins TT8 interact with MYB proteins in the presence of a WD40 repeat containing protein TTG1, forming a transcriptional regulation complex that activates anthocyanin biosynthetic genes [47]. We confirmed the physical interaction between MabHLH11 and MaMYB4 in Y2H and BiFC assays (Fig. 4). Overexpression of MabHLH11 individually or together with its interacting MaMYB4 in *M. albus* hairy roots also activated scopolin biosynthesis, resulting in substantial scopolin accumulation, suggesting that scopolin accumulation is regulated via direct physical interaction between MabHLH11 and MaMYB4. Upregulated MaMYB4 exerted a large effect on the relative expression level of MabHLH11, whereas upregulated MabHLH11 showed little effect on MYB4 expression (Fig. 5C, D), suggesting that MaMYB4 is an upstream regulatory transcription factor of MabHLH11. Scopolin levels were sharply increased by MabHLH11 and

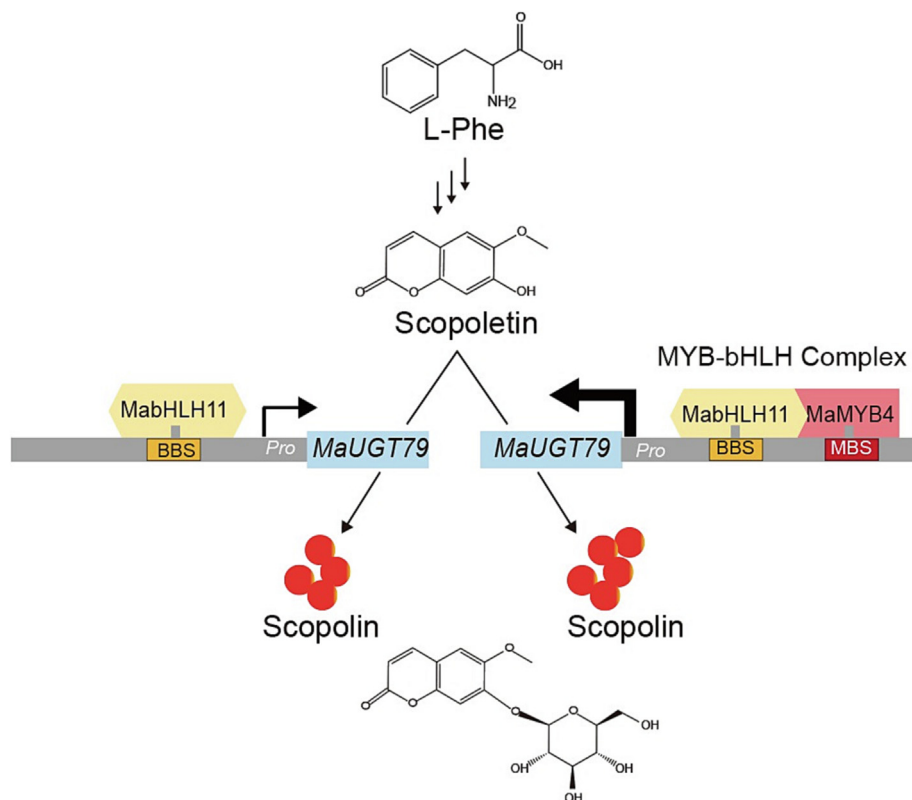


Fig. 8. Proposed regulation model of MabHLH11- and MaMYB4-mediated scopolin biosynthesis in *M. albus*. MabHLH11 activates the expression of the scopolin biosynthesis gene *MaUGT79* to induce scopolin accumulation. This activation is further reinforced by MabHLH11 and MaMYB4 interaction, which amplified the regulation by activating the promoters of *MaUGT79*, resulting in much higher accumulation of scopolin. MBS, MYB binding sites; BBS, bHLH binding sites.

MaMYB4 co-expression (Fig. 5D), suggesting that interaction between MabHLH11 and MaMYB4 exerts an additive regulation effect on scopolin accumulation in *M. albus*.

4.3. MabHLH11 coupled with MaMYB4 to induce the expression of *MaUGT79*

MabHLH11 is a positive regulator of scopolin biosynthesis in *M. albus*. However, it is still not clear which structural genes are the target genes of MabHLH11. In our study, we found 3 MYC cis-acting elements in the promoter of *MaUGT79* (Fig. S5), and MabHLH11 acts by binding to the promoter of *MaUGT79* (Fig. 6). This finding is consistent with a previous finding [48] that most bHLH proteins bind to sites that contain a CA-TG consensus. The MBW complex's specificity for multiple target genes probably depends on the participation of bHLH and their R2R3-MYB partners [15]. In our study, MabHLH11 interacting with MaMYB4 similarly activated the scopolin biosynthetic genes *MaUGT79* and *MaCCoAOMT*. The expression levels of *MaUGT79* and *MaCCoAOMT* were increased with overexpression of MabHLH11 or MaMYB4 hairy roots and they were synergistically activated in MabHLH11-MaMYB4 co-expression hairy roots compared with those in EV. In addition, promoter transactivation assay showed that the *MaUGT79* gene involved in scopolin biosynthesis was activated by MabHLH11 and the activation was increased by the presence of MaMYB4 (Fig. 7C). In the presence of both MabHLH11 and MaMYB4, the expression of *MaUGT79* increased > 1.28-fold relative to that under MabHLH11 alone, indicating that the specificity of target promoter recognition by MabHLH11 and the partner MaMYB4. This result is consistent with a previous finding [49] that MYB- and bHLH-binding cis-elements in the promoters of structural genes are required for bHLH TF binding. In *M. truncatula*, the bHLH

transcription factors TSAR1 and TSAR2 bind to the G-box (CACGTG) present in the promoters of HMGR involved in triterpene saponin biosynthesis [46]. We also identified putative MYB binding sites (MBS) and bHLH-binding sites (BBS) in the *MaUGT79* promoter (Fig. 7A). Thus, the *MaUGT79* promoter was activated by MabHLH11 in combination with MaMYB4.

A model of the inferred interactions of MabHLH11 and MaMYB4 and their regulatory roles in scopolin biosynthesis in *M. albus* is presented in Fig. 8. MabHLH11 alone bound the promoter of the scopolin structural gene and activated its expression. The increased expression of the structural gene ultimately promoted the accumulation of scopolin.

Our study has elucidated the little-studied molecular regulatory mechanism of MabHLH11-MaMYB4 in scopolin accumulation in *M. albus*. The hierarchical regulatory model of scopolin biosynthesis provides a theoretical basis for molecular biological study of research on scopolin biosynthesis and of mechanisms of response to environmental stresses.

Data availability

The genomic sequence of *M. albus* is available at NCBI (NCBI BioProject ID PRJNA674670).

CRediT authorship contribution statement

Zhen Duan: Investigation, Data curation, Writing – original draft. **Shengsheng Wang:** Data curation, Resources. **Zhengshe Zhang:** Data curation, Formal analysis. **Qi Yan:** Data curation, Formal analysis. **Caibin Zhang:** Methodology. **Pei Zhou:** Data curation, Formal analysis. **Fan Wu:** Writing – review & editing. **Jiyu**

Zhang: Writing – review & editing, Funding acquisition, Supervision.

Declaration of competing interest

The authors declare that they have no known competing financial interests or personal relationships that could have appeared to influence the work reported in this paper.

Acknowledgments

This work was financially supported by the National Natural Science Foundation of China (32061143035, 32271752), Inner Mongolia Seed Industry Science and Technology Major Demonstration Project (2022JBG0040), and the Fundamental Research Funds for the Central Universities (Izujbky-2022-ey17).

Appendix A. Supplementary data

Supplementary data for this article can be found online at <https://doi.org/10.1016/j.cj.2023.06.011>.

References

- [1] S. Doll, M. Kuhlmann, T. Rutten, M.F. Mette, S. Scharfenberg, A. Petridis, D.C. Berreth, H.P. Mock, Accumulation of the coumarin scopolin under abiotic stress conditions is mediated by the *Arabidopsis thaliana* THO/TREX complex, *Plant J.* 93 (2018) 431–444.
- [2] I.A. Stringlis, R. de Jonge, C.M. Pieterse, The age of coumarins in plant-microbe interactions, *Plant Cell Physiol.* 60 (2019) 1405–1419.
- [3] M.J.E.E.E. Voges, Y. Bai, P. Schulze-Lefert, E.S. Sattely, Plant-derived coumarins shape the composition of an *Arabidopsis* synthetic root microbiome, *Proc. Natl. Acad. Sci. U. S. A.* 116 (2019) 12558–12565.
- [4] C. Alonso, I.M. Garcia, N. Zapata, R. Perez, Variability in the behavioural responses of three generalist herbivores to the most abundant coumarin in *Daphne laureola* leaves, *Entomol. Exp. Appl.* 132 (2009) 76–83.
- [5] H.H. Tsai, W. Schmidt, Mobilization of iron by plant-borne coumarins, *Trends Plant Sci.* 22 (2017) 538–548.
- [6] K. Robe, G. Conejero, F. Gao, L. Lefebvre-Legendre, E. Sylvestre-Gonon, V. Rofidal, S. Hem, N. Rouhier, M. Barberon, A. Hecker, F. Gaymard, E. Izquierdo, C. Dubos, Coumarin accumulation and trafficking in *Arabidopsis thaliana*: a complex and dynamic process, *New Phytol.* 229 (2021) 2062–2079.
- [7] E. Park, C.G. Lee, J. Kim, E. Lim, S. Yeo, S.Y. Jeong, Scopolin prevents adipocyte differentiation in 3T3-L1 preadipocytes and weight gain in an ovariectomized obese mouse model, *Int. J. Mol. Sci.* 21 (2020) 8699.
- [8] J. Siwinska, L. Kadzinski, R. Banasiuk, A. Gwizdek-Wisniewska, A. Olry, B. Banecki, E. Lojkowska, A. Ilnatowicz, Identification of QTLs affecting scopolin and scopoletin biosynthesis in *Arabidopsis thaliana*, *BMC Plant Biol.* 14 (2014) 280.
- [9] Y. Deng, S. Lu, Biosynthesis and regulation of phenylpropanoids in plants, *Crit. Rev. Plant Sci.* 36 (2017) 257–290.
- [10] X. Liu, P. Zhang, Q. Zhao, A.C. Huang, Making small molecules in plants: a chassis for synthetic biology-based production of plant natural products, *J. Integr. Plant Biol.* 65 (2023) 417–443.
- [11] K. Robe, E. Izquierdo, F. Vignols, H. Rouached, C. Dubos, The coumarins: secondary metabolites playing a primary role in plant nutrition and health, *Trends Plant Sci.* 26 (2021) 248–259.
- [12] C. Gachon, R. Baltz, P. Saindrenan, Over-expression of a scopoletin glucosyltransferase in *Nicotiana tabacum* leads to precocious lesion formation during the hypersensitive response to tobacco mosaic virus but does not affect virus resistance, *Plant Mol. Biol.* 54 (2004) 137–146.
- [13] H.H. Tsai, J. Rodríguez-Celma, P. Lan, Y.C. Wu, I.C. Vélez-Bermúdez, W. Schmidt, Scopoletin 8-hydroxylase-mediated fraxetin production is crucial for iron mobilization, *Plant Physiol.* 177 (2018) 194–207.
- [14] Y. Liu, K. Ma, Y. Qi, G. Lv, X. Ren, Z. Liu, F. Ma, Transcriptional regulation of anthocyanin synthesis by MYB-bHLH-WDR complexes in kiwifruit (*Actinidia chinensis*), *J. Agric. Food Chem.* 69 (2021) 3677–3691.
- [15] A. Feller, K. Machemer, E.L. Braun, E. Grotewold, Evolutionary and comparative analysis of MYB and bHLH plant transcription factors, *Plant J.* 66 (2011) 94–116.
- [16] P.C. Bailey, C. Martin, G. Toledo-Ortiz, P.H. Quail, E. Huq, M.A. Heim, M. Jakoby, M. Werber, B. Weisshaar, Update on the basic helix-loop-helix transcription factor gene family in *Arabidopsis thaliana*, *Plant Cell* 15 (2003) 2497–2502.
- [17] W. Xu, C. Dubos, L. Lepiniec, Transcriptional control of flavonoid biosynthesis by MYB-bHLH-WDR complexes, *Trends Plant Sci.* 20 (2015) 176–185.
- [18] X.C. Wang, J. Wu, M.L. Guan, C.H. Zhao, P. Geng, Q. Zhao, *Arabidopsis* MYB4 plays dual roles in flavonoid biosynthesis, *Plant J.* 101 (2020) 637–652.
- [19] R. Gao, T. Han, H. Xun, X. Zeng, P. Li, Y. Li, Y. Wang, Y. Shao, X. Cheng, X. Feng, J. Zhao, L. Wang, X. Gao, Q. Zhao, MYB transcription factors GmMYB2 and GmMYB8 function in a feedback loop to control pigmentation of seed coat in soybean, *J. Exp. Bot.* 72 (2021) 4401–4418.
- [20] D. Schenke, C. Boettcher, D. Scheel, Crosstalk between abiotic ultraviolet-B stress and biotic (flg22) stress signalling in *Arabidopsis* prevents flavonol accumulation in favor of pathogen defence compound production, *Plant Cell and Environ.* 34 (2011) 1849–1864.
- [21] F. Gao, K. Robe, M. Bettembourg, N. Navarro, V. Rofidal, V. Santoni, F. Gaymard, F. Vignols, H. Roschzttardtz, E. Izquierdo, C. Dubos, The transcription factor bHLH121 interacts with bHLH105 (ILR3) and its closest homologs to regulate iron homeostasis in *Arabidopsis*, *Plant Cell* 32 (2020) 508–524.
- [22] F. Gao, K. Robe, F. Gaymard, E. Izquierdo, C. Dubos, The transcriptional control of iron homeostasis in plants: a tale of bHLH transcription factors?, *Front Plant Sci.* 10 (2019) 6.
- [23] S.A. Kim, I.S. LaCroix, S.A. Gerber, M.L. Guerinot, The iron deficiency response in *Arabidopsis thaliana* requires the phosphorylated transcription factor URI, *Proc. Natl. Acad. Sci. U. S. A.* 116 (2019) 24933–24942.
- [24] R. Lei, Y. Li, Y. Cai, C. Li, M. Pu, C. Lu, Y. Yang, G. Liang, bHLH121 functions as a direct link that facilitates the activation of FIT by bHLH IVC transcription factors for maintaining Fe homeostasis in *Arabidopsis*, *Mol. Plant* 13 (2020) 634–649.
- [25] A. Petridis, S. Döll, L. Nichelmann, W. Bilger, H.P. Mock, *Arabidopsis thaliana* G2-Like flavonoid regulator and brassinosteroid enhanced expression 1 are low-temperature regulators of flavonoid accumulation, *New Phytol.* 211 (2016) 912–925.
- [26] J.M. Zabala, L. Marinoni, J.A. Giavedoni, G.E. Schrauf, Breeding strategies in *Melilotus albus* Desr., a salt-tolerant forage legume, *Euphytica* 214 (2018) 22.
- [27] P.M. Evans, G.A. Kearney, *Melilotus albus* (Medik.) is productive and regenerates well on saline soils of neutral to alkaline reaction in the high rainfall zone of south-western Victoria, *Aust. J. Exp. Agric.* 43 (2003) 349–355.
- [28] J. Zhang, H. Di, K. Luo, Z. Jahufer, F. Wu, Z. Duan, A. Stewart, Z. Yan, Y. Wang, Coumarin content, morphological variation, and molecular phylogenetics of *Melilotus*, *Molecules* 23 (2018) 810.
- [29] F. Wu, Z. Duan, P. Xu, Q.I. Yan, M. Meng, M. Cao, C.S. Jones, X. Zong, P. Zhou, Y. Wang, K. Luo, S. Wang, Z. Yan, P. Wang, H. Di, Z. Ouyang, Y. Wang, J. Zhang, Genome and systems biology of *Melilotus albus* provides insights into coumarins biosynthesis, *Plant Biotechnol. J.* 20 (2022) 592–609.
- [30] K. Luo, F. Wu, D. Zhang, R. Dong, Z. Fan, R. Zhang, Z. Yan, Y. Wang, J. Zhang, Transcriptomic profiling of *Melilotus albus* near-isogenic lines contrasting for coumarin content, *Sci. Rep.* 7 (2017) 4577.
- [31] F. Wu, K. Luo, Z. Yan, D. Zhang, Q. Yan, Y. Zhang, X. Yi, J. Zhang, Analysis of miRNAs and their target genes in five *Melilotus albus* NILs with different coumarin content, *Sci. Rep.* 8 (2018) 14138.
- [32] L. Chen, F. Wu, J. Zhang, NAC and MYB families and lignin biosynthesis-related members identification and expression analysis in *Melilotus albus*, *Plants* 10 (2021) 303.
- [33] Z. Duan, Q. Yan, F. Wu, Y. Wang, S. Wang, X. Zong, P. Zhou, J. Zhang, Genome-wide analysis of the UDP-Glycosyltransferase family reveals its roles in coumarin biosynthesis and abiotic stress in *Melilotus albus*, *Int. J. Mol. Sci.* 22 (2021) 10826.
- [34] J. Xu, H. Xu, H. Zhao, H. Liu, L. Xu, Z. Liang, Genome-wide investigation of bHLH genes and expression analysis under salt and hormonal treatments in *Andrographis paniculata*, *Ind. Crop Prod.* 183 (2022) 114928.
- [35] C. Chen, H. Chen, Y. Zhang, H.R. Thomas, M.H. Frank, Y. He, R. Xia, TBtools: an integrative toolkit developed for interactive analyses of big biological data, *Mol. Plant* 13 (2020) 1194–1202.
- [36] S. Kumar, G. Stecher, K. Tamura, MEGA7: molecular evolutionary genetics analysis version 7.0 for bigger datasets, *Mol. Biol. Evol.* 33 (2016) 1870–1874.
- [37] M.A. Heim, M. Jakoby, M. Werber, C. Martin, B. Weisshaar, P.C. Bailey, The basic helix-loop-helix transcription factor family in plants: a genome-wide study of protein structure and functional diversity, *Mol. Biol. Evol.* 20 (2003) 735–747.
- [38] S. Wang, Z. Duan, Q. Yan, F. Wu, P. Zhou, J. Zhang, Genome-wide identification of the GRAS family genes in *Melilotus albus* and expression analysis under various tissues and abiotic stresses, *Int. J. Mol. Sci.* 23 (2022) 7403.
- [39] F. Jeanmougin, J.D. Thompson, M. Gouy, J.G. Higgins, T.J. Gibson, Multiple sequence alignment with Clustal X, *Trends Biochem. Sci.* 23 (1998) 403–405.
- [40] X. Zong, S. Wang, Y. Han, Q. Zhao, P. Xu, Q. Yan, F. Wu, J. Zhang, Genome-wide profiling of the potential regulatory network of lncRNA and mRNA in *Melilotus albus* under salt stress, *Environ. Exp. Bot.* 189 (2021) 104548.
- [41] X. Liu, R. Wu, S.M. Bulley, C. Zhong, D. Li, KiwiFit MYB51-like and GBF3 transcription factors influence L-ascorbic acid biosynthesis by activating transcription of *GDP-L-galactose phosphorylase 3*, *New Phytol.* 234 (2022) 1782.
- [42] Q. Zeb, X. Wang, C. Hou, X. Zhang, M. Dong, S. Zhang, Q. Zhang, Z. Ren, W. Tian, H. Zhu, The interaction of CaM7 and CNGC14 regulates root hair growth in *Arabidopsis*, *J. Integr. Plant Biol.* 62 (2020) 887–896.
- [43] S. Wang, Z. Duan, J. Zhang, Establishment of hairy root transformation system of *Melilotus albus* induced by *Agrobacterium rhizogenes*, *Acta Agraria Sin.* 29 (2021) 2591–2599.
- [44] H. Zheng, L. J. Jing, X. Jiang, C. Pu, S. Zhao, J. Yang, J. Guo, G. Cui, J. Tang, Y. Ma, M. Yu, X. Zhou, M. Chen, C. Lai, L. Huang, Y. e. Shen, The ERF-VII transcription factor SmERF73 coordinately regulates tanshinone biosynthesis in response to stress elicitors in *Salvia miltiorrhiza*, *New Phytol.* 231 (2021) 1940–1955.
- [45] N.Q. Dong, H.X. Lin, Contribution of phenylpropanoid metabolism to plant development and plant-environment interactions, *J. Integr. Plant Biol.* 63 (2021) 180–209.

- [46] J. Mertens, J. Pollier, R. Vanden Bossche, I. Lopez-Vidriero, J.M. Franco-Zorrilla, A. Goossens, The bHLH transcription factors TSAR1 and TSAR2 regulate triterpene saponin biosynthesis in *Medicago truncatula*, *Plant Physiol.* 170 (2016) 194–210.
- [47] C.Q. Yang, X. Fang, X.M. Wu, Y.B. Mao, L.J. Wang, X.Y. Chen, Transcriptional regulation of plant secondary metabolism, *J. Integr. Plant Biol.* 54 (2012) 703–712.
- [48] T.K. Blackwell, L. Kretzner, E.M. Blackwood, R.N. Eisenman, H. Weintraub, Sequence-specific DNA binding by the c-Myc protein, *Science* 250 (1990) 1149–1151.
- [49] R. Rajput, J. Naik, R. Stracke, A. Pandey, Interplay between R2R3 MYB-type activators and repressors regulates proanthocyanidin biosynthesis in banana (*Musa acuminata*), *New Phytol.* 236 (2022) 1108–1127.